Innovative Absorber/Stripper Configurations for CO_2 Capture by Aqueous Monoethanolamine

Majeed S. Jassim[†] and Gary T. Rochelle*[,‡]

Department of Chemical Engineering, University of Bahrain, P.O. Box 32038, Bahrain, and Department of Chemical Engineering, The University of Texas at Austin, Austin, Texas 78712

The state-of-the-art technology to capture CO_2 from coal-fired power plants is absorption/stripping with aqueous monoethanolamine (MEA). The energy consumption in stripping can be 15−30% of the power-plant output. A rigorous rate-based model for CO_2−MEA−H_2O was used to simulate several flowsheet alternatives that reduce the energy requirement using Aspen Plus with RateFrac. Results were calculated for vapor recompression, multipressure, and simple strippers at 5 and 10 °C approach temperatures and 70, 90, and 95% CO_2 removal. The "equivalent work of steam/mole of CO_2 removed" and the reboiler duty were used to compare the proposed schemes and to show the shift of energy use from work to heat. The total equivalent work for multipressure was less than that for the simple stripper by 0.03−0.12 GJ/(ton of CO_2), and the reboiler duty was less by 0.15−0.41 GJ/(ton of CO_2). The multipressure with vapor recompression is an attractive option because it utilizes the overhead water vapor latent heat to reduce reboiler duty load, recovers the work of compression to strip more CO_2, and shows more reversible behavior.

1. Introduction

CO_2 capture and sequestration is an important option for reducing the greenhouse emissions that cause climate change. Absorption/stripping with aqueous chemical solvents such as alkanolamines and promoted potassium carbonate are well-known and effective technologies for removing CO_2.

These existing and mature technologies are energy-intensive and use large quantities of moderate level heat. The energy consumption in the stripper reboiler is estimated to be 15−30% of the net power production of a coal-fired power plant. CO_2 emissions from coal-fired power plants were 2 279.3 million metric tons in 2003 and contribute 32.4% of total CO_2 emission in the US Energy Information Administration (EIA)[1] report.

Figure 1 shows the configuration of a conventional absorption/stripping amine process. The concentration of carbon dioxide in the flue gas stream from a coal-fired power plant is 10−12%. Aqueous 30 wt % monoethanolamine (MEA) removes carbon dioxide in a countercurrent contactor. The solvent is regenerated at 100−120 °C in a simple, countercurrent, reboiled stripper operated at a single pressure, usually 1−2 atm. The rich solvent feed is preheated by cross-exchange with hot lean solvent product to within 5−30 °C of the stripper bottoms. The overhead vapor is cooled to condense water, which is returned as reflux to the countercurrent stripper. When used for CO_2 sequestration and other applications, the product CO_2 is compressed to 100−200 atm.

Freguia and Rochelle[2] used Aspen Plus with RateFrac to model a simple absorption/stripping process with CO_2−MEA−H_2O. The process simulator was used to optimize the validated base case by varying design and process parameters. Both Singh et al.[3] and Desideri and Paolucci[4] applied the Aspen Plus environment to simulate the classical amine flowsheet, and they showed that high capital and operating costs are associated with the introduction of an MEA amine-treating unit in a coal-fired power plant.

The economics and feasibility of this process depends on the energy consumption in the stripper. Therefore, minimization of the reboiler duty should be the primary objective for any suggested modifications to the existing traditional flowsheet.

Energy efficiency can be enhanced by recovery of useful heat from the overhead condenser. The overhead vapor can contain 1−5 mol of water vapor for every 1 mol of CO_2. In vapor recompression, the overhead vapor would be compressed by a factor of 2−10 and then exchanged with the bottoms liquid to provide heat for the reboiler.

This paper further develops the concepts of vapor recompression and multipressure stripping. Rigorous evaluations of these suggested flowsheet modifications are compared to the simple arrangement using Aspen Plus simulation modules for CO_2 absorption by aqueous 30 wt % MEA. Optimization of these proposed flowsheets is carried out to reduce the process total energy requirement. We also explain in detail the advantages of the vapor recompression and multipressure concepts and the shift of energy use from heat to work.

2. Modeling

2.1. Thermodynamic Model. The knowledge of vapor−liquid equilibria (VLE) is important in understanding the design of separation processes, determining the driving forces, and identifying the molecular and ionic speciation in the bulk liquid phase. Austgen and co-workers[5,6] regressed the available data on CO_2 solubility in aqueous MEA to develop a rigorous and thermodynamically consistent model. He determined the binary interaction parameters to represent the activity coefficients within the electrolyte-NRTL framework that was developed by Chen et al.[7] and modified by Mock et al.[8] In a later publication, Jou et al.[9] produced better solubility data for CO_2 in a 30 wt % MEA aqueous solution for a wide range of temperatures and pressures and explained the errors of previous publications.

Freguia and Rochelle[2] improved Austgen's[2] VLE model with a new set of regressed interaction parameters generated in Aspen Plus using the solubility data of Jou et al.[9] In this work, we have used the thermodynamic model developed by Freguia and Rochelle.[2]

* To whom correspondence should be addressed. Tel.: (512) 471-7230. Fax: (512) 475-7824. E-mail: gtr@che.utexas.edu.
[†] University of Bahrain.
[‡] The University of Texas at Austin.

10.1021/ie050547s CCC: $33.50
Published on Web 11/15/2005

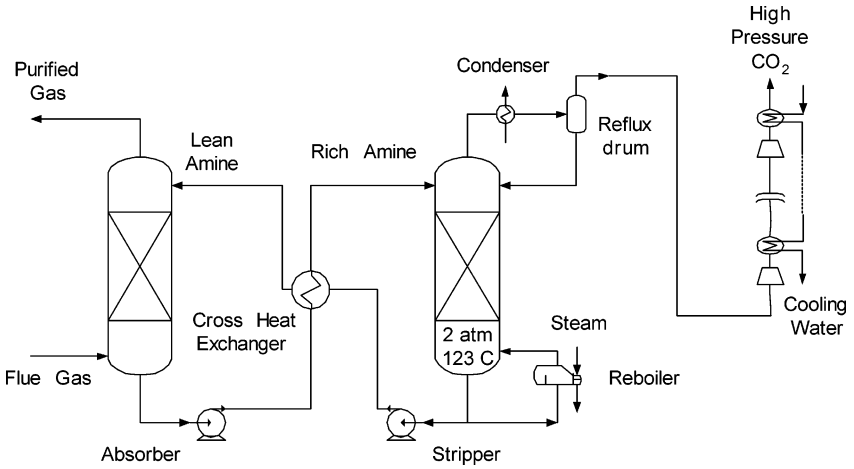

Figure 1. Simple absorption/stripping.

2.2. Kinetic Model. We have used the Freguia and Rochelle[2] framework and reactor parameters to model the MEA system. The absorber performance is modeled by a combination of equilibrium and kinetic reactions, while the stripper performance is modeled only by equilibrium reactions. The details of these reactions and the rate constant expressions can be found in Freguia and Rochelle.[2]

Freguia[10] developed a Fortran rate routine for the absorber model to work around two fluxes in RateFrac. RateFrac incorrectly uses two-film theory to calculate CO_2 mass transfer enhancement by averaging the interface and bulk reaction rates. For the simple reaction kinetics, RateFrac uses concentration-based driving forces rather than activity-based driving forces in the computation of species fluxes; this creates inconsistency with the electrolyte-NRTL thermodynamic framework.

Freguia[10] wrote a Fortran subroutine with the interface pseudo-first-order (IPFO) approximation to estimate CO_2 mass transfer with fast chemical reactions. This concept assumes that rapid CO_2 depletion occurs in a thin sublayer next to the interface while the other species have constant concentrations. The IPFO model was used to analytically solve flux equations simultaneously. The subroutine used correlations by Onda et al.,[11] Weiland,[12] and Pacheco[13] to compute wetted area, density, and CO_2 diffusivity. It also utilized experimental wetted-wall column data by Dang[14] to adjust the MEA−CO_2 rate constant. The subroutine interacts with the RateFrac absorber module to characterize the bulk and boundary layer kinetics until a correct analytical solution is reached. Table 1 shows RateFrac built-in models that are used to calculate thermodynamic and transport properties for liquid and gas phases.

We have detected a minor bug in the Freguia and Rochelle[2] absorber model, because accurate representation of mass transfer with chemical reaction requires artificial kinetics to be defined in the user routine. Unfortunately, the same routine is used to define kinetics in the bulk solution. The artificial kinetics gives a reaction rate of CO_2 to bicarbonate which is too slow to give equilibrium in the bulk solution. At a typical rich loading of 0.45 (mol of CO_2)/(mol of MEA), the artificial kinetics gives a HCO_3^- loading of 0.010 mol/(mol of MEA) compared to 0.044 with a true equilibrium. Because the HCO_3^- loading is low in either case, this deficiency should have a minimum effect on the predicted energy requirements.

3. Flowsheet Descriptions and Rationales

The details of the flue gas and the chemical solvent are summarized in Table 2. The carbon dioxide in the flue gas is typical of a coal-fired power plant. The maximum strength of the chemical solvent (MEA) is limited to 30 wt % due to corrosion restrictions. The design characteristics of the base case absorber and stripper are summarized in Table 3. The cross-exchanger approach temperature was varied between 5 and 10 °C. The following sections describe the simple absorption/stripping process and three proposed flowsheets with different

Table 1. Built-in Thermodynamic and Transport Correlations Used by RATEFRAC

properties	phase distribution	model
	thermodynamic	
fugacity	liquid	electrolyte-NRTL
	vapor	Redlich−Kwong
enthalpy	liquid	electrolyte-NRTL
	vapor	Redlich−Kwong
	transport	
density	liquid	electrolyte-NRTL
	vapor	Redlich−Kwong
viscosity	liquid	Jones−Dole
	vapor	Chapman−Enskog−Brokaw
surface tension	liquid	Hakim−Steinberg−Stiel with Onsager−Samaras correction
diffusion coefficient	liquid	Nernst−Hartley
	vapor	Chapman−Enskog−Wike−Lee
thermal conductivity	liquid	Sato−Riedel
	vapor	Wassiljema−Mason−Saxena

Table 2. Typical Characteristics of Flue Gas and Chemical Solvent

flue gas	
composition (mol %)	CO_2: 12.33, H_2O: 9.40
absorber inlet (°C)	55
absorber pressure drop (atm)	0.1
inlet flow (after saturation) (kmol/m^2·s)	0.08
fresh chemical solvent	30 wt % MEA at 40 °C

Table 3. Design Characteristics of the Absorber and the Stripper

absorber	
packing height (m)	15
pressure drop (kPa)	10
packing type	random, metal, CMR#2
packing liquid holdup (%)	0.01
cross-exchanger approach (°C)	5, 10
stripper	
packing height (m)	10
diameter (m)	4.5
bottom pressure (atm)	2
pressure drop (atm)	0.1
reboiler	equilibrium
rich solvent feed location (m)	0.5 (from top)
packing type	random, metal, CMR#2
packing liquid holdup (%)	4

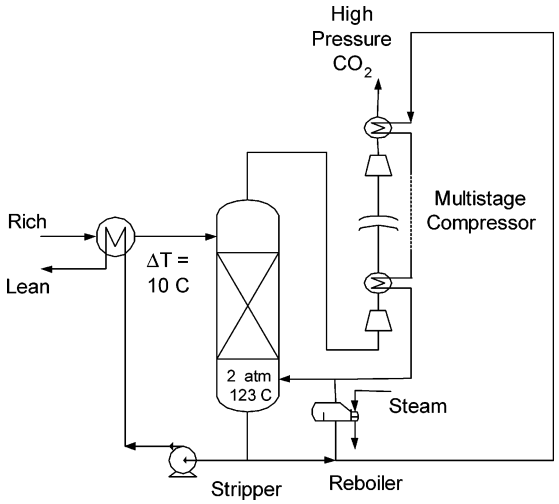

Figure 2. Simple stripping with vapor recompression.

modes of energy integration in order to reduce the energy consumption in the absorption/stripping system.

3.1. Simple Absorption/Stripping. A conventional, simple process consists of two main mass transfer unit operations: an absorber and a stripper, as shown in Figure 1. The composition of the flue gas represents that of a typical coal-fired power plant but without NO_x or SO_2 because these should be removed by pretreating. The flue gas feed rate to the amine plant was 0.08 kmol/(m^2•s) or 3.05 kmol/s (after saturation) from a 500 MW coal-fired power plant. The 30 wt % MEA countercurrently interacts with flue gas in a 7 m diameter absorber randomly packed with 15 m of Cascade mini rings (CMR#2). The stripper is 4.5 m in diameter and packed with 10 m of CMR#2.

The CO_2-rich solvent is regenerated in a simple, countercurrent stripper with a reboiler at 2.0 atm and 115−120 °C. The vapor top product is cooled to condense water which is refluxed. The carbon dioxide product is compressed to 136.2 atm for sequestration in a five-stage compressor intercooled to 40 °C. The compressor was designed with a maximum compression ratio in each stage of 3 and a maximum temperature of 350 °F. The compressors were modeled with 79.5% polytropic efficiency using the Gas Processors Supplier Association (GPSA) method.

3.2. Simple Absorption/Stripping with Vapor Recompression. With vapor recompression as shown in Figure 2, the knockout drum is removed and the stripper bottom is used to intercool the gas stream in the multistage compressor to 130 °C, except for the last two compressor stages, as the CO_2 was cooled to 35 °C. The purpose of vapor recompression is to recover the heat of condensation of the overhead water vapor and the heat of compression by reboiling the stripper. The number of compressor stages for this scenario was doubled to 10 in order to satisfy the maximum temperature restriction, and as a consequence, the pressure ratio was reduced to 1.45.

3.3. Multipressure Stripping (MP). The multipressure stripper is represented by Figure 3. This system integrates the stripper with the first two stages of a nine-stage compressor. The first two stages are used to increase the pressure in the stripper. The stripper operates at three pressure levels: 5 m of the packing is at 2 atm, 2.5 m is at 2.8 atm, and 2.5 m is at 4 atm. Performance was also calculated by 2/3.1/5 atm with a similar packed depth. The rationale for such a distribution is to allow sufficient mass transfer in the bottom half of the stripper and then evenly divide the upper half. The vapor from a lower-pressure zone is withdrawn to a compressor stage and then reinjected at the next-higher-pressure zone up the column. This model assumes that all pressure levels were in the same vessel with a diameter of 4.5 m, but an alternative design could put each pressure level into a separate vessel. The overhead top stripper vapor at 4 atm was further compressed in six stages intercooled to 40 °C.

3.4. Multipressure Stripping with Vapor Recompression. The multipressure stripper with vapor recompression is illustrated in Figure 4. This process is similar to case 2 except that the stripper is integrated with compressors as in the multipressure (MP) stripper case. The stripper overhead vapor is not cooled but instead is routed directly to nine compressor stages. As in case 2, the vapor is cooled to 40 °C before it is further compressed to the supercritical state.

4. Results

Table 4 presents a summary of 24 optimized cases for all four stripper configurations at 70, 90, and 95% CO_2 removal and with 5 or 10 °C approach temperatures. The approach

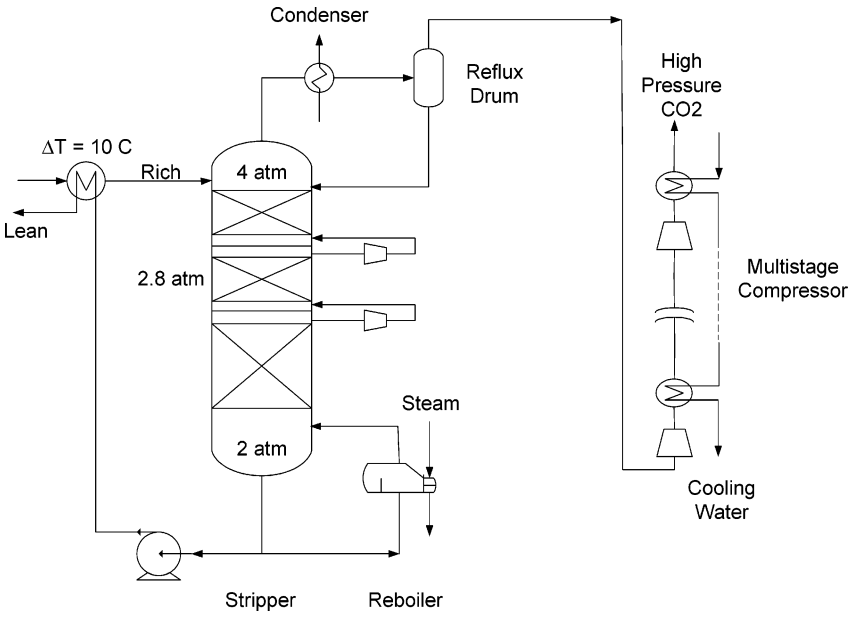

Figure 3. Multipressure stripping.

Table 4. Details of Optimized Scenarios

CO_2 rem. (%)	ΔT (°C)	config.[a]	lean loading ((mol CO_2)/(mol MEA))	rich loading ((mol CO_2)/(mol MEA))	reboiler duty GJ/(ton of CO_2)	reboiler duty normalized	compressors work (GJ/(ton CO_2))	total work (GJ/(ton CO_2))	CO_2 capacity ((mol CO_2)/(kg solvent))	absorber dia. (m)	stripper dia. (m)
70	5	simple	0.249	0.478	3.85	0.90	0.32	1.00	1.10	8	4.5
		simple_VR	0.232	0.479	2.02	0.47	0.64	1.00	1.19	7	4.5
	10	simple	0.232	0.479	4.02	0.94	0.32	1.03	1.19	8	4.5
		simple_VR	0.232	0.479	2.43	0.57	0.62	1.05	1.19	8	4.5
	5	MP2_5	0.285	0.474	2.84	0.66	0.38	0.90	0.96	7.5	4.5
		MP2_5_VR	0.285	0.474	2.27	0.53	0.48	0.90	0.96	7.5	4.5
	10	MP2_5	0.249	0.477	3.13	0.73	0.40	0.96	0.75	7.5	4.5
		MP2_5_VR	0.249	0.477	2.62	0.61	0.50	0.97	0.75	7.5	4.5
90	5	simple	0.249	0.459	4.08	0.95	0.32	1.04	1.01	8	4.5
		simple_VR	0.249	0.459	2.10	0.49	0.66	1.04	1.01	8	4.5
	10	simple	0.249	0.459	4.29	1.00	0.32	1.08	1.00	8	4.5
		simple_VR	0.214	0.458	2.45	0.57	0.64	1.08	1.19	7	4.5
	5	MP2_4	0.338	0.465	3.16	0.74	0.38	0.94	0.58	8	4.5
		MP2_4_VR	0.338	0.465	2.49	0.58	0.50	0.95	0.58	8	4.5
	10	MP2_4	0.249	0.455	3.35	0.78	0.45	1.05	0.96	7.5	4.5
		MP2_4_VR	0.249	0.455	2.64	0.62	0.57	1.05	0.96	7.5	4.5
	5	MP2_5	0.338	0.465	3.00	0.70	0.42	0.96	0.58	8	4.5
		MP2_5_VR	0.338	0.465	2.47	0.58	0.51	0.97	0.58	8	4.5
	10	MP2_5	0.249	0.455	3.15	0.74	0.51	1.09	1.07	7.5	4.5
		MP2_5_VR	0.249	0.455	2.60	0.61	0.62	1.10	1.07	7.5	4.5
95	5	simple	0.338	0.462	4.10	0.96	0.32	1.03	0.57	8	5
		simple_VR	0.338	0.462	2.38	0.56	0.63	1.06	0.57	8	5
	10	simple	0.232	0.440	4.51	1.05	0.32	1.12	1.00	8	5
		simple_VR	0.232	0.440	2.57	0.60	0.66	1.11	1.00	8	5

[a] MP = multipressure, VR = vapor recompression.

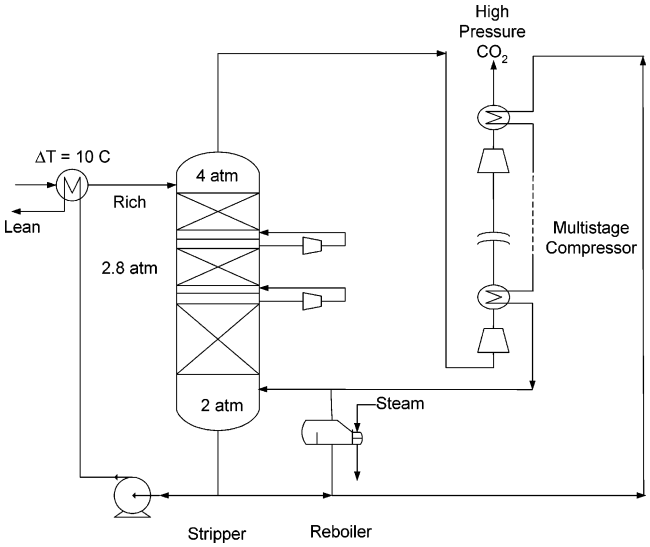

Figure 4. Multipressure stripping with vapor recompression.

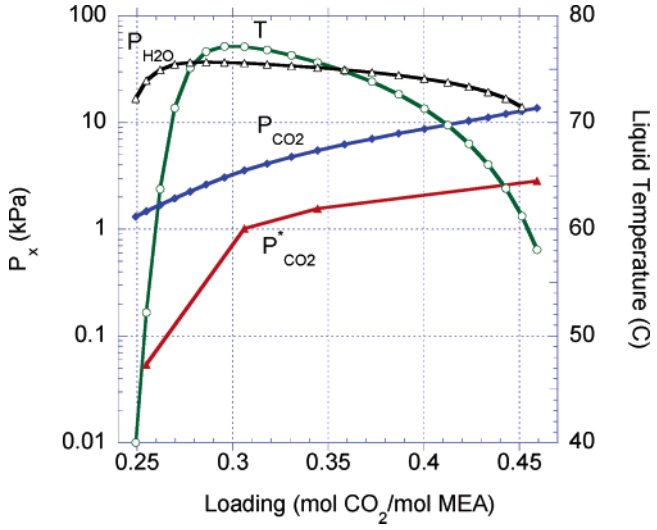

Figure 5. Absorber performance profiles for low lean loading (0.249 mol/mol), 90% CO_2 removal, L/G = 3.9 kg/kg.

temperature is the temperature difference between the stripper bottom stream (lean solution) and the hot rich solution that is fed to the stripper. The total equivalent work for each case was minimized by varying lean loading.

4.1. Absorber Performance. Figures 5 and 6 show the distribution of CO_2 partial pressure (P_{CO_2}), equilibrium CO_2 partial pressure ($P^*_{CO_2}$), temperature, and water partial pressure (P_{H_2O}) across the absorber with two common values of lean loading. The temperature and P_{H_2O} were strongly correlated. The exothermic absorption of CO_2 resulted in a greater temperature in the middle of the absorber than at either end. With a lower lean loading and L/G (Figure 5), the maximum temperature was 77 °C and located near the top of the column. With a greater lean loading and L/G, the maximum temperature was 64 °C near the bottom of the absorber. The closest approach to CO_2 saturation is at the bottom of the absorber with a high lean loading, but it occurs near the maximum temperature in the top one-third of the column with the low lean loading. The equilibrium partial pressure of CO_2 is never >20% of the operating partial pressure.

4.2. Simple Stripper Performance. Figure 7 shows the McCabe−Thiele diagram for the simple stripper case with 90% removal, 5 °C approach, and optimized lean loading of 0.249. The bottom 10 sections of the column have a desorption driving force varying from 15 to 20 kPa. The top 7 sections are tightly pinched at the rich end of the column. Figure 8 shows the McCabe−Thiele diagram at the same conditions but at a lean loading of 0.392. It is clear that the richer solution requires only 4 segments before the rich-end pinch. The reason for such behavior could be attributed to the smaller loading difference across the length of the stripper and the higher driving forces.

4.3. Multipressure Stripper Performance. The McCabe−Thiele diagram for the 2/2.8/4 atm multipressure stripper with 90% removal, 10 °C approach, and an optimized lean loading

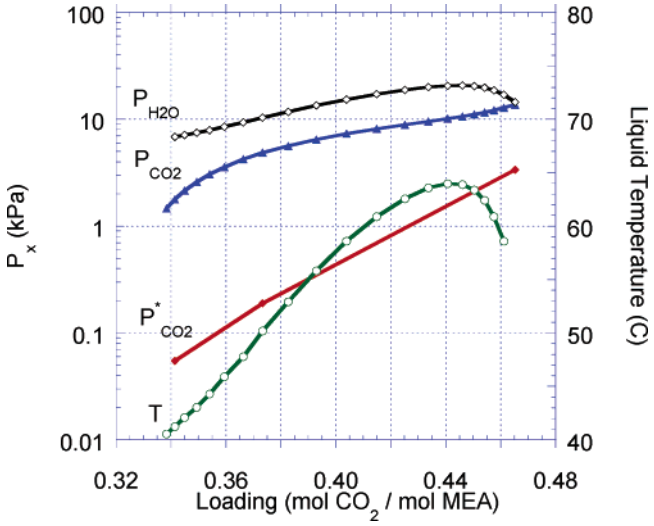

Figure 6. Absorber performance profiles for high lean loading (0.338 mol/mol), 90% CO_2 removal, $L/G = 9.5$ kg/kg.

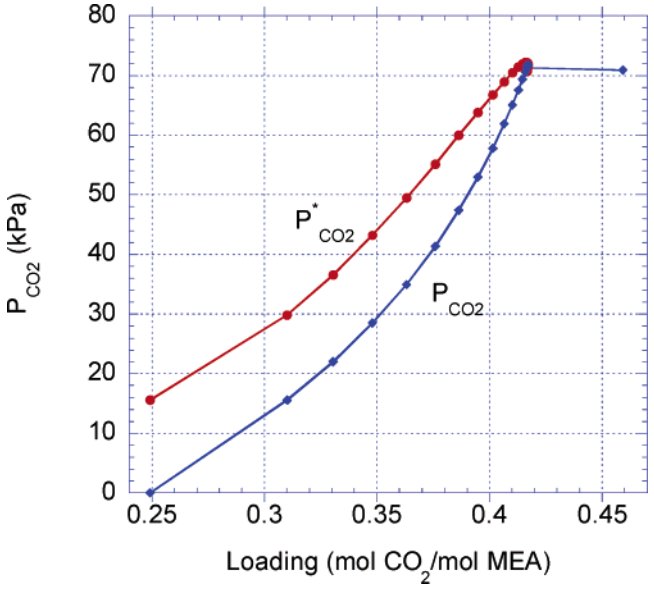

Figure 7. Stripper McCabe−Thiele diagram for simple absorption/stripping, optimized lean loading (0.249 mol/mol), 90% CO_2 removal, 5 °C approach.

of 0.249 is given in Figure 9. The operating and equilibrium lines pinch at the top of the column (similar to the simple case) and at the two compressor positions. The existence of pinches suggests a more-reversible operation.

4.4. Comparison of Multipressure and Simple Stripper. Figure 10 compares the liquid temperature profile in the simple stripper with liquid and vapor temperature profiles in the 2/2.8/4 atm multipressure stripper with 90% CO_2 recovery, 10 °C approach temperature, and optimized 0.249 lean loading. The liquid temperature of the simple stripper is constant for almost the upper half of the column and then increases to a maximum of 123 °C in the reboiler. The multipressure stripper is more nearly isothermal. The inclusion of compressors results in a sharp temperature increase as the vapor is withdrawn from segments 6 and 11 and compressed before it is reintroduced in segments 5 and 10. This enthalpy of compression is transferred to the countercurrent and incoming rich amine solution. The temperature of the aqueous solution suddenly drops as it flashes when passing from each higher-pressure section to the lower one.

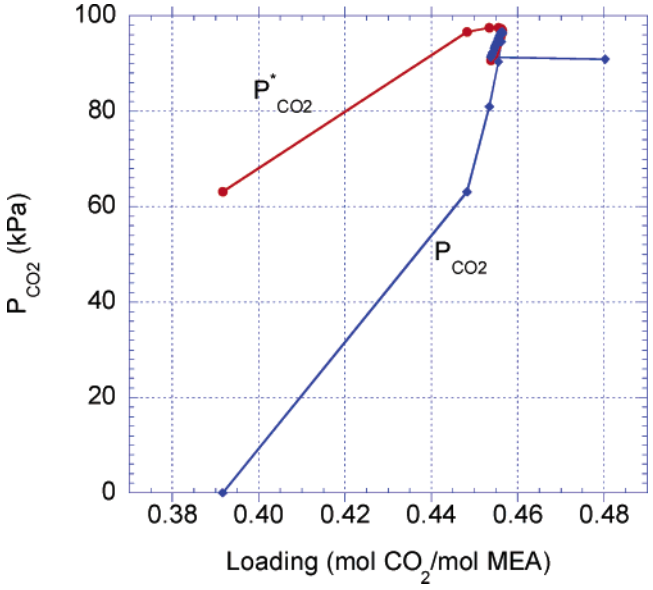

Figure 8. Stripper McCabe−Thiele diagram for simple absorption/stripping, optimized lean loading (0.392 mol/mol), 90% CO_2 removal, 5 °C approach.

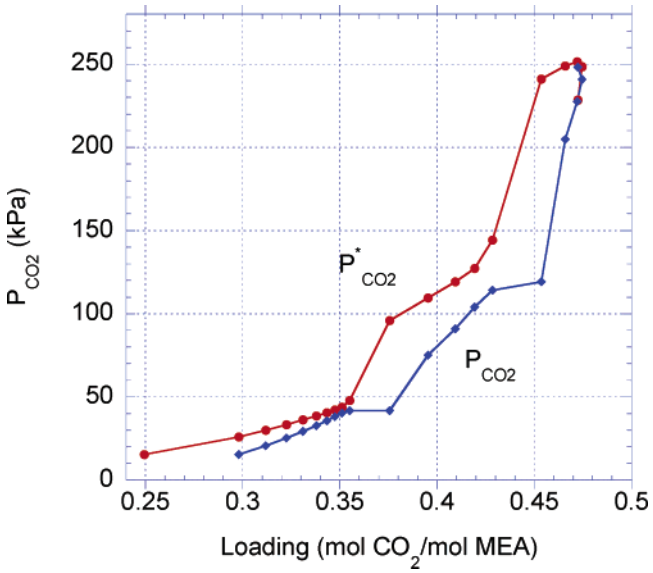

Figure 9. Stripper McCabe−Thiele diagram for multipressure stripping at 2/2.8/4 atm, optimized lean loading (0.249 mol/mol), 90% CO_2 removal, 10 °C approach.

Figure 11 shows how the ratio of CO_2 to water vapor varies across the simple and 2/2.8/4 atm multipressure strippers for 90% CO_2 removal, 10 °C approach, and optimized lean loading of 0.249 mol/mol. For the simple stripper case, the ratio increases to a maximum value of 0.7 (mol of CO_2)/(mol of H_2O). In the multipressure stripper, less water vapor leaves with the CO_2. The successive compression of the vapor causes the water to condense and the CO_2/H_2O ratio to increase to at the stripper exit, 1.7 versus only 0.7 for the simple case. The condensing water provides heat that reduces the reboiler heat duty.

Figure 9 shows the McCabe−Thiele diagram of the 2/2.8/4 atm multipressure stripper. There are three pinches across the stripper in comparison to only one pinch in the simple case (Figures 7 and 8). The driving forces are smaller and more distributed than in the simple case; hence, the multipressure case is more reversible.

4.5. Optimization. The overall work of the system is the combination of work and heat elements in the system: pump work, compressor work, and reboiler heat duty (eq 1). The

Table 5. Optimization of 2/2.8/4 atm Multipressure Stripper with Vapor Recompression at 5 and 10 °C Approach with 90% CO_2 Removal

				work (GJ/ton CO_2)						
lean loading (mol CO_2/mol MEA)	rich loading (mol CO_2/mol MEA)	stripper bottom T (°C)	CO_2 capacity (mol CO_2/kg solvent)	pumps	compressors $\Delta T = 5$ °C	compressors $\Delta T = 10$ °C	reboiler $\Delta T = 5$ °C	reboiler $\Delta T = 10$ °C	total $\Delta T = 5$ °C	total $\Delta T = 10$ °C
0.427	0.489	109	0.28	0.09	0.48	0.50	0.49	0.70	1.06	1.29
0.338	0.465	118	0.58	0.04	0.50	0.50	0.41	0.53	0.95	1.07
0.249	0.455	123	0.92	0.03	0.59	0.57	0.37	0.45	0.99	1.05
0.143	0.469	125	1.61	0.02	0.96	0.97	0.29	0.36	1.27	1.35

Table 6. Optimization of Simple Stripper with Vapor Recompression at 5 and 10 °C Approach with 90% CO_2 Removal

				work (GJ/ton CO_2)						
lean loading (mol CO_2/mol MEA)	rich loading (mol CO_2/mol MEA)	stripper bottom T (°C)	CO_2 capacity (mol CO_2/kg solvent)	pumps	compressors $\Delta T = 5$ °C	compressors $\Delta T = 10$ °C	reboiler $\Delta T = 5$ °C	reboiler $\Delta T = 10$ °C	total $\Delta T = 5$ °C	total $\Delta T = 10$ °C
0.427	0.486	109	0.28	0.06	0.56	0.54	0.48	0.69	1.10	1.29
0.338	0.465	118	0.59	0.04	0.63	0.60	0.39	0.51	1.06	1.15
0.249	0.459	123	1.00	0.02	0.66	0.63	0.36	0.44	1.04	1.09
0.143	0.469	125	1.45	0.01	0.83	0.81	0.32	0.37	1.16	1.19

equivalent work is the common basis to treat heat and work combinations using Carnot cycle efficiency for the heat. It is assumed that the heat is delivered 10 °C higher than the stripper bottom temperature and the heat sink is 40 °C. The efficiency of the Carnot cycle was assumed to be 75% (eq 2). At our typical steam conditions, this is equivalent to a 66% isentropic efficiency for a simple steam turbine condensing at 40 °C.

$$\text{total work} = \sum(\text{pumps}) + \sum(\text{compressors}) + \text{reboiler work} \quad (1)$$

$$\text{reboiler work} = Q_r\left(\frac{T_b + 10 - 40}{T_b + 10 + 273}\right) \times 0.75 \quad (2)$$

where Q_r is the reboiler heat duty (MJ/(kg of CO_2) or GJ/(ton of CO_2)) and T_b is the stripper bottom temperature (°C).

The multipressure stripper pump has a discharge pressure of 6.5 atm and the simple stripper pump has a discharge pressure of 4.5 atm in order to overcome the cross-exchanger pressure drop and stripper height and to deliver the rich solution at the top column pressure. The absorber pump has a discharge pressure of 3 atm. The pump efficiency is 65% for all cases.

Figure 12 shows how the total work varies with lean loading in the 2/2.8/4 atm multipressure stripper with vapor recompression and 90% removal. The cases with 5 °C approach give 5.6−18.0% lower total work than the cases with 10 °C approach. In both cases, the total work has local minima at lean loadings of 0.25 and 0.34 mol/mol. However, the global minimum occurs at 0.25 with the 10 °C approach and 0.34 with the 5 °C approach.

Tables 5 and 6 explain the mechanism of the double minima for the 2/2.8/4 multipressure and simple strippers, respectively. The work of the compressor increases with the leaner solution because it has higher CO_2 capacity, while the reboiler duty decreases with the leaner solution because it has to overcome less driving forces in order to desorb CO_2. The leaner solution requires less circulation rates, and thus, less work is delivered by the pumps. At 0.34 mol/mol loading and 5 °C approach, the ratio of compressor-to-reboiler work in the simple case has reduced from 1.6 to 1.2 in the multipressure case, and that created another minimum. The position of minima at different approach temperatures is dependent on the reboiler duty because the changes in the compressor and pump works are negligible.

4.6. Vapor Recompression. According to Table 7, vapor recompression reduces the reboiler duty by 49 and 21% compared to the simple and multipressure cases. The reboiler duty of the multipressure stripper is less than that of the simple stripper by 22%. The vapor recompression increases the compressor work by 102 and 97% for the simple stripper and by 33 and 28% for 2/2.8/4 atm multipressure at 5 and 10 °C approaches, respectively. However, it is observed that vapor recompression with multipressure provides 30 and 12% less work than the simple stripper with vapor recompression at 5 and 10 °C approaches, respectively. The total equivalent work of the multipressure scheme is lower than that of the simple scheme by 3 and 8% for the 10 and 5 °C approaches, respectively. However, it is noted that vapor recompression did not have an effect on the total equivalent work.

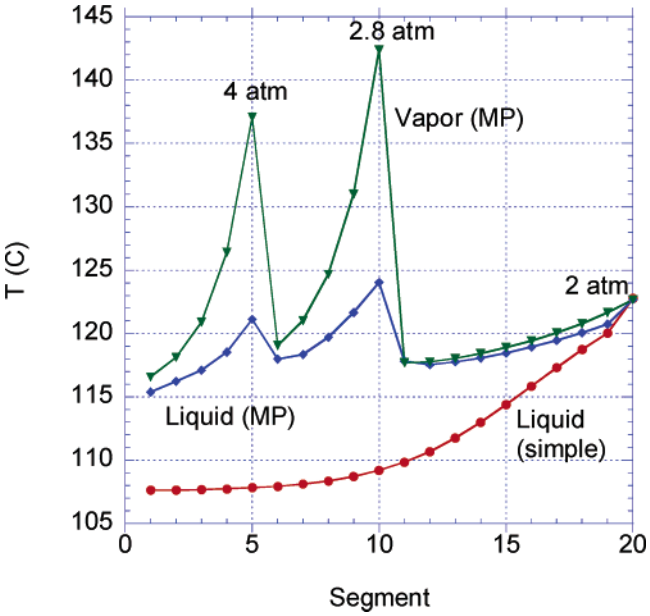

Figure 10. Temperature profile in simple and multipressure strippers: optimized lean loading (0.249 mol/mol), 90% CO_2 removal, 10 °C approach.

According to Table 4, the simple configuration with vapor recompression at 70% CO_2 removal and 5 °C approach has the lowest reboiler duty with 2.02 GJ/(ton of CO_2). The lowest total equivalent work of 0.9 GJ/(ton of CO_2) is achieved by both cases of 2/3.1/5 atm multipressure at 70% CO_2 removal and 5 °C approach. The pressure distribution of 2/2.8/4 atm in the multipressure stripper is better than 2/3.1/5 atm because it requires 3−4% less total equivalent work.

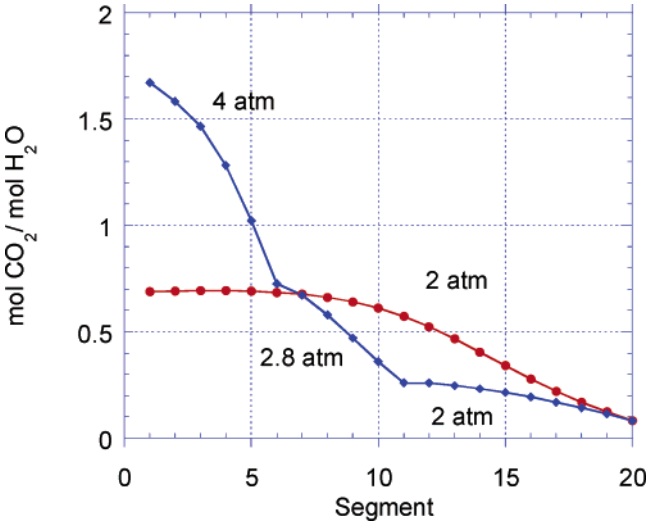

Figure 11. CO_2/H_2O profile in simple and multipressure strippers: optimized lean loading (0.249 mol/mol), 90% CO_2 removal, 10 °C approach.

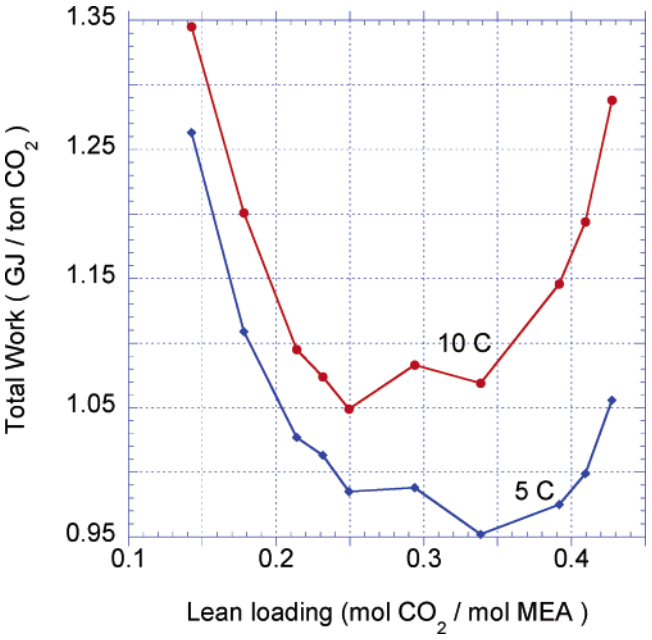

Figure 12. Optimization of a 2/2.8/4 atm multipressure stripper with vapor recompression for 90% CO_2 removal.

Table 7. Comparison of Total Equivalent Work and Reboiler Duty for 90% CO_2 Recovery

case	approach temp (°C)	equivalent work (GJ/ton CO_2)	reboiler duty (GJ/ton CO_2)
simple	5	1.04	4.08
	10	1.08	4.29
simple VR	5	1.04	2.10
	10	1.08	2.45
MP 2/2.8/4	5	0.94	3.16
	10	1.05	3.35
MP 2/2.8/4 VR	5	0.95	2.49
	10	1.05	2.64

5. Conclusions

Both vapor recompression and multipressure stripping shift energy use from heat to work. This can be advantageous because it is more convenient and flexible to exploit the electric grid to run the compressors than to use the heat from the existing steam-turbine system to run the reboiler, and hence, this causes less disruption to the existing operation. These CO_2 capture schemes could be attractive with a strategy to shut down CO_2 capture during periods of peak electricity demand.

Multipressure stripping requires 3−11% less equivalent work than simple stripping, especially if used with a lower approach temperature. Multipressure stripping utilizes the latent heat of the overhead water vapor to reduce reboiler duty load and recovers the work of compression to strip more CO_2 within the column. It also showed more reversible behavior because it had multiple pinches with more distributed and smaller driving forces. Vapor recompression provides no reduction in the equivalent work requirement.

Using a 5 °C approach rather than 10 °C in the cross exchanger provides a saving of 0.03−0.12 GJ/(ton of CO_2) of total equivalent work and 0.15−0.41 GJ/(ton of CO_2) of the reboiler duty relative to 10 °C approach.

With a 5 °C approach, the optimized cyclic loading was as low as 0.13 (mol of CO_2)/(mol of MEA). This is significantly less than the 0.21−0.25 mol/mol obtained with a 10 °C approach, typical of industrial practice.

These results have been used by Trimeric Corporation to prepare capital and operating cost estimates for a 500 MW coal-fired power plant.[15] The CO_2 capture economics showed that simple stripper with vapor recompression, multipressure, and multipressure with vapor recompression reduced the cost of CO_2 removal ($/ton) by 4.6, 9.8, and 8.4%, respectively, relative to the simple stripper.

Acknowledgment

This paper was prepared with the support of the U.S. Department of Energy (DOE), under Award No. DE-FC26-02NT41440. However, any opinions, findings, conclusions, or recommendations expressed herein are those of the authors and do not necessarily reflect the views of the DOE. M.S.J. is grateful to the Fulbright Exchange Scholar Program. We are grateful to Kevin S. Fisher and Carrie Beitler from Trimeric Corporation for their technical discussions. We extend our appreciation to Aspen Technology for providing the software.

Literature Cited

(1) *Emissions of Greenhouse Gases in the United States*; Energy Information Administration: Washington, DC, 2003. ftp://ftp.eia.doe.gov/pub/oiaf/1605/cdrom/pdf/ggrpt/057303.pdf.

(2) Freguia, S.; Rochelle, G. T. Modeling of CO_2 capture by aqueous monoethanolamine. *AIChE J.* **2003**, *49*, 1676−1686.

(3) Singh, D.; Croiset, E.; Douglas, P. L.; Douglas, M. A. Techno-economic study of CO_2 capture from an existing coal-fired power plant: MEA scrubbing vs O_2/CO_2 recycle combustion. *Energy Convers. Manage.* **2003**, *44*, 3073−3091.

(4) Desideri, U.; Paolucci, A. Performance modeling of a carbon dioxide removal system for power plants. *Energy Convers. Manage.* **1999**, *40*, 1899−1915.

(5) Austgen, D. M. A model for vapor−liquid equilibria for acid gas−alkanolamine−water systems. Ph.D. Dissertation, The University of Texas at Austin, Austin, TX, 1989.

(6) Austgen, D. M.; Rochelle, G. T.; Peng, X.; Chen, C. C. Model of vapor−liquid equilibria for aqueous acid gas−alkanolamine systems using the electrolyte-NRTL equation. *Ind. Eng. Chem. Res.* **1989**, *28*, 1060−1073.

(7) Chen, C. C.; Britt, H. I.; Boston, J. F.; Evans, L. B. Extension and application of the Pitzer equation for vapor−liquid equilibrium of aqueous electrolyte systems with molecular solutes. *AIChE J.* **1979**, *25*, 820−831.

(8) Mock, B.; Evans, L. B.; Chen, C. C. Thermodynamic Representation of Phase Equilibria of Mixed-Solvent Electrolyte Systems. *AIChE J.* **1986**, *32*, 1655−1664.

(9) Jou, F.-Y.; Mather, A. E.; Otto, F. D. Solubility of CO_2 in a 30 mass percent monoethanolamine solution. *Can. J. Chem. Eng.* **1995**, *73*, 140−147.

(10) Freguia, S. Modeling of CO_2 Removal from Flue Gases with Monoethanolamine. M.Sc. Thesis, The University of Texas at Austin, Austin, TX, 2002.

(11) Onda, K.; Sada, E.; Takeuchi, H. Gas absorption with chemical reaction in packed columns. *J. Chem. Eng. Jpn.* **1968**, *1*, 62−66.

(12) Weiland, R. H. *Physical Properties of MEA, DEA, MDEA and MDEA-Based Blends Loaded with CO_2*; GRI/GPA Research Report RR-152; Gas Processors Association: Tulsa, OK, 1996.

(13) Pacheco, M. A. Mass Transfer, Kinetics and Rate-Based Modeling of Reactive Absorption. Ph.D. Dissertation, The University of Texas at Austin, Austin, TX, 1998.

(14) Dang, H. Carbon Dioxide Absorption Rate and Solubility in Monoethanolamine/Piperazine/Water. M.Sc. Thesis, The University of Texas at Austin, Austin, TX, 2000.

(15) Fisher, K. S.; Jassim, M.; Rochelle, G.; Beitler, C.; Rueter, C.; Searcy, K., Figueroa, J. Integrating Monoethanolamine (MEA) Regeneration with CO_2 Compression to Reduce CO_2 Capture Costs. Presented at 4th Annual Conference on Carbon Capture and Sequestration, Alexandria, VA, May 2−5, 2005; Paper 38.

Received for review May 11, 2005
Revised manuscript received October 10, 2005
Accepted October 12, 2005

IE050547S